Level widths and level densities in ^{28}Si, ^{46}Ti, ^{52}Cr, and ^{60}Ni from Ericson fluctuations

Americo Salas-Bacci, Steven M. Grimes, Thomas N. Massey, Yannis Parpottas,
Raymond T. Wheeler, and James E. Oldendick
Ohio University, Athens, Ohio 45701, USA
(Received 4 March 2004; published 26 August 2004)

Ericson fluctuations in the differential cross sections were investigated for the compound reactions ^{27}Al$(p,n_0)^{27}$Si, ^{45}Sc$(p,n_4)^{45}$Ti, ^{45}Sc$(p,n_5)^{45}$Ti, ^{51}V$(p,n_0)^{51}$Cr, and ^{59}Co$(p,n_0)^{59}$Ni. Level widths in the compound nuclei ^{28}Si, ^{46}Ti, ^{52}Cr, and ^{60}Ni were extracted from the analysis of the differential cross sections by the Fourier method and a nonlinear fit to the $\ln\langle A_k^2+B_k^2\rangle$ distribution. The neutron spectra for each reaction were measured at least at three backward angles but the coherence width $\langle\Gamma\rangle$ did not show a strong angular dependence. Nuclear level densities for the above nuclei were extracted by relating the average level spacing $D^{J\pi}$ to the average level width $\Gamma^{J\pi}$ using the fluctuation theory. Reasonable agreements were found with other level densities and level density compilations based in the Fermi gas formalism of Al-Quraishi and Huang for ^{28}Si, ^{46}Ti, and ^{52}Cr but the comparison diverges for ^{60}Ni for which additional measurements are required in order to clarify the observed discrepancies. The level density parameters that best describe the data are $a=3.5$ and $\delta=4.0$, $U<25$ MeV, for ^{28}Si, $a=4.8$ and $\delta=-0.3$, $U<20$ MeV, for ^{46}Ti, and $a=4.8$ and $\delta=0.3$, $U<20$ MeV, for ^{52}Cr.

DOI: 10.1103/PhysRevC.70.024311 PACS number(s): 21.10.Ma

I. INTRODUCTION

Measurements of differential cross sections with high energy resolution exhibit fluctuations as a function of energy if the reaction mechanism is not completely direct. The study of these fluctuations leads to the extraction of level width in the continuum and this in turn to the determination of level density. The level density information is obtained from the compound nucleus rather than from the residual nuclei.

The average level width in the continuum, $\langle\Gamma\rangle$, also known as the coherence width or level width, can be found by the powerful and elegant method of Fourier expansion of the differential cross section. This is described in Sec. III, Measurement of Level Width. In turn, the determination of level density with one parity approximation is presented in Sec. IV, Evaluation of Level Density, where we also introduce a comparison with other level densities and with the most recent nuclear level densities (NLD) compilations. Good energy resolution is required in order to study Ericson fluctuations; the techniques used for achieving this are described in Sec. II. An additional condition $\langle\Gamma\rangle/\langle D\rangle>1$, where $\langle D\rangle$ is the average spacing between levels, is fulfilled by the present data as can be observed from the plots of level densities.

II. EXPERIMENTAL DESCRIPTION

To measure coherence width in the compound nucleus for the determination of nuclear level density we used the Ohio University 4.5 MV Tandem Van de Graaff Accelerator. Protons were accelerated to produce (p,n) reactions in ^{27}Al, ^{45}Sc, ^{51}V, and ^{59}Co. The information about the coherence width can be inferred from the neutron measurements but these were limited to low energy neutrons in order to obtain good energy resolution. The neutron time-of-flight facility is composed of a beam swinger and a 30 meter flight path, which is suitable for Ericson fluctuation studies and is shown in Fig. 1. Differential cross sections can be measured at different angles from 0° to 162° by rotating the swinger around its axis of rotation while keeping the neutron detector fixed. For time-of-flight experiments a very short time spread ($\leqslant$2 nsec) can be accomplished by chopping and then bunching the beam. Projectile bursts with a period from 200 to 12800 nsec can be obtained by a proper chopping frequency selection given by $f=5/2^n$ MHz, where n goes from 0 to 6.

The proton beam emerging from the swinger passed through two tantalum collimators of diameters 1/4 and 1/8 inch before entering an electrically isolated scattering chamber. Secondary electrons produced by collisions with the internal pipe that connected the mouth of the chamber with the end of the swinger were suppressed by a ring kept at −300 V. The current collected by the target holder, tantalum stopping plate and scattering chamber were added and digitized by a beam current integrator. The sides of the scattering

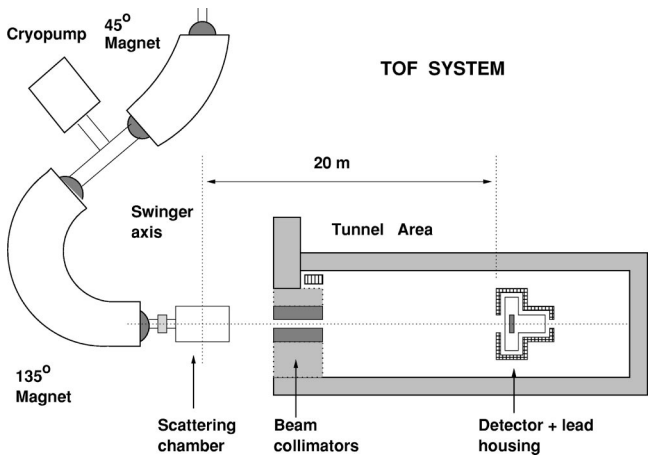

FIG. 1. TOF System: Swinger and tunnel area.

TABLE I. Targets used in the experiment.

Target	Reaction	Thickness mg/cm^2	$\langle E_p \rangle$ MeV	Δ keV
Al	^{27}Al$(p,n)^{27}$Si	13.5	7.40	600
Sc	^{45}Sc$(p,n)^{45}$Ti	4.0	5.20	200
V	^{51}V$(p,n)^{51}$Cr	4.4	3.10	500
Co	^{59}Co$(p,n)^{59}$Ni	4.4	3.40	260

chamber are 1.25 cm thick except for an area of the central wall which is only 2 mm thick. The purpose of this thinner wall is to reduce the neutron attenuation for (p,n) reactions in the side wall of the chamber while products of other (p,z) reactions were completely stopped there. To produce good shielding and background reduction in the tunnel area, a set of blocks of polyethylene, lead, and tungsten were used to collimate gammas and neutrons between the scattering chamber and the entrance to the tunnel.

Self supporting natural targets of Al, Sc, V, and Co with a purity of 99.9+% were used in the experiment. The target thickness and proton energy loss for typical incident proton energies are shown in Table I.

A detector chosen to reduce noise and random pulses was used to study fluctuations in the cross section. It consisted of a 170 mm diameter Bicron BC-408 plastic scintillator, 2.54 cm thick. Three Hamamatsu photomultipliers were attached to the plastic scintillator through specially shaped light pipes, as can be seen in Fig. 2. The anode signals from the lateral photomultipliers were added by a logic OR gate and, in conjunction with the central photomultiplier anode pulse, were sent to the coincidence AND gate. The output of the coincidence circuit was the START signal for the time-of-flight experiment, while the STOP signal came from a capacitive beam pickoff unit, located 5 cm above the mouth of the scattering chamber. To reduce the effect of natural or artificial radioactivities on the time independent background, and gammas produced by (n,γ) reactions in the cast concrete of the tunnel, the whole detector system was surrounded by a 5 inch thick enclosure of lead bricks with openings at the entrance of the detector window and also at the end of the main photomultiplier.

The energy resolution, $\sigma_E = \pm 2E\sqrt{(\sigma_x/x)^2+(\sigma_t/t)^2}$, that is, the error associated with the kinetic energy E, is shown in Fig. 3 for different flight paths from 5 to 30 m; σ_x is the uncertainty in the neutron flight path x arising principally from the finite thickness of the detector and σ_t is related to the time resolution Δt by $\Delta t = 2.35\sigma_t$. Figure 3 assumes a $\sigma_{t\gamma} = 1.0$ nsec and includes the transit time for neutrons in a 2.54 cm thick detector. As is evident from the resolution equation, a good energy resolution is accomplished with a long flight path and low neutron energy. An estimation of the level width for the compound nuclei in this study restricts the energy resolution such that $\sigma_E \leqslant 5$ keV. At the same time this imposes a restriction on both the detector position and neutron energy. Under these conditions the detector was positioned at 20 meters obtaining a 4 keV average energy resolution for neutrons in the energy range 1.0 to 1.7 MeV.

The absolute efficiency needed for calculating the differential cross section has been measured using the thick target neutron energy spectrum of the reaction ^{9}Be(p,n) with 5.0 MeV protons at 0°. The binned counts were calibrated with respect to the neutron flux obtained for the same reaction, energy and angle [1] that was measured relative to the ^{27}Al(d,n) reaction, $E_d = 7.44$ MeV at 120° which was measured accurately with a ^{235}U fission chamber [2]. Figure 4 shows the detector efficiency for two different runs exhibiting the same shape variation with energy; these minima and maxima in the absolute efficiency are strongly correlated with resonances in the cross section for air and aluminum (scattering chamber) in the range of neutron energies of the present study. The error in the absolute efficiency is $\sim \pm 0.005$ for this range. The influence of the efficiency in the analysis of the fluctuating cross section is important in the large energy scale but different from the rapid variations of the Ericson fluctuations.

III. MEASUREMENT OF LEVEL WIDTH

A. Differential cross section. Thick target equation

The neutron spectra were subjected to background subtraction, converted to time, neutron kinetic energy, binned, and by inverse kinematics each bin was transformed to proton kinetic energy. The differential cross section equation including the relation between the proton kinetic energy bin ΔE and the energy loss in the differential target thickness Δx is given in Ref. [3] by:

$$\frac{d\sigma}{d\Omega} = \frac{A_w Ze}{P_{iso} N_a Q_t \epsilon_{abs}} \frac{\Delta C}{\Delta E \Delta \Omega} \frac{1}{\rho} \frac{dE}{dx}, \tag{1}$$

where N_a is the Avogadro's number, A_w the atomic weight, P_{iso} the isotopic abundance (0-1), Q_t the total charge, ϵ_{abs} the

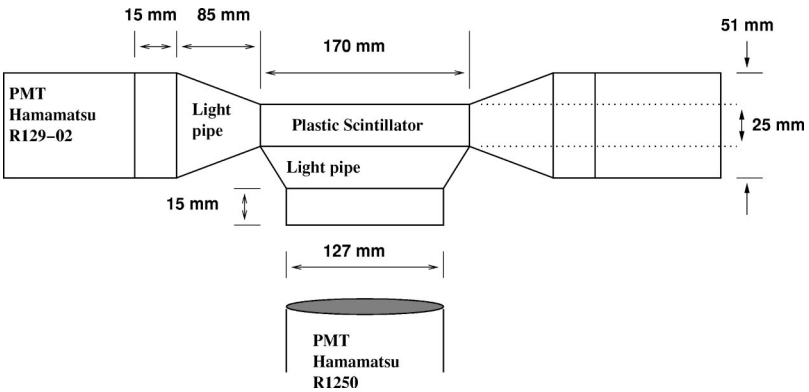

FIG. 2. Upper side view of detector.

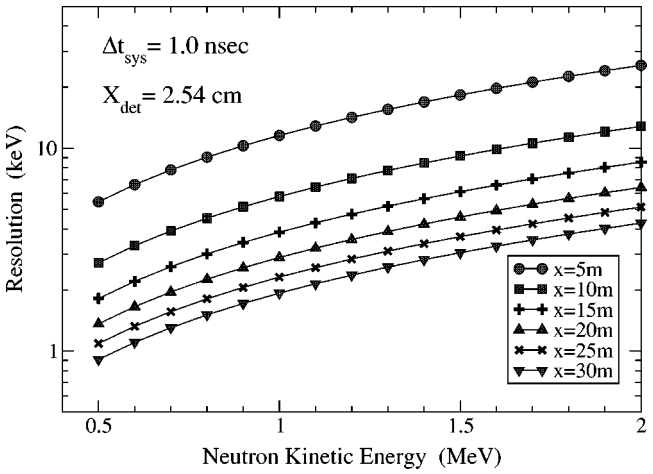

FIG. 3. Neutron energy resolution for different flight paths.

absolute efficiency, Ze the projectile charge state, and ΔC the binned counts. The energy loss term $1/\rho\, dE/dx$ was calculated with the SRIM program [4]. Figure 5 shows the fluctuations in the cross section as predicted by Ericson [5], calculated using Eq. (1).

If we consider E_p as the incident proton energy and the total energy loss in the thick target as Δ (see Table I), then the range of proton energies available is E_p, $E_p-\Delta$. This range of energies excites many energy levels of the compound nucleus between U, $U-\Delta$ which decay emitting, among other particles, neutrons in the range $\sim E_n$, $E_n-\Delta$. Given the high energy resolution of the experiment the information on the level density is contained in the fluctuations of the neutron spectrum such that each δE_n, the size of the energy resolution, is related with a δE_p by kinematical relations, as it is finally expressed in Eq. (1). In the experiment we should avoid the overlapping between adjacent levels, and with this limitation we have measured the neutron spectrum with different proton energies related by $E_p'=E_p\pm\frac{2}{3}\Delta$ and overlapped the different spectra to finally obtain the differential cross section as is shown in Fig. 5. In summary, the Δ values indicate that each separate measurement gave an excitation function over about 200 keV (Sc, Co) and

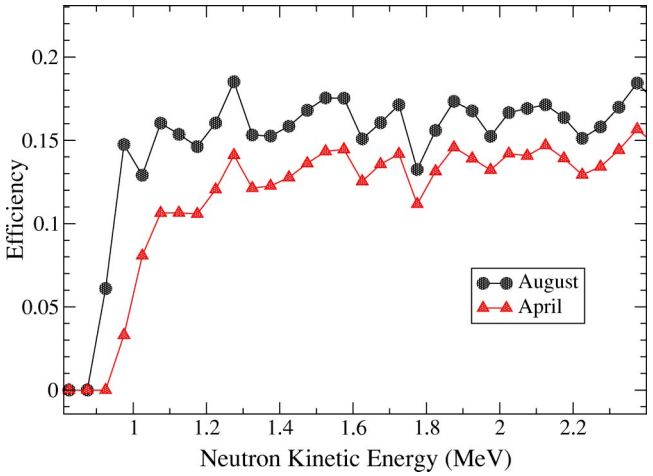

FIG. 4. Efficiency for August and April experiments.

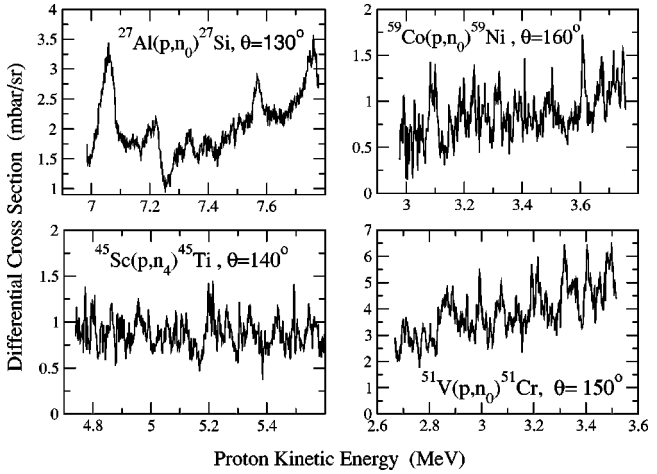

FIG. 5. Differential Cross Sections showing the Ericson fluctuations.

500 keV (Al, V). The resolution of the measurement was determined by the time of flight resolution and it was ~4 keV. A comparison of the present differential cross section with energy bins similar to the resolution measurement of Deconninck [6] shows a very good agreement for the reaction $^{51}\mathrm{V}(p,n_0)^{51}\mathrm{Cr}$.

B. Fourier analysis of fluctuating excitation function

It is attributed to Böhning [7] that an expansion in Fourier series of the fluctuating excitation function results in the determination of the coherence width $\langle\Gamma\rangle$:

$$\frac{d\sigma}{d\Omega}=\sum_{k=0}^{M}\left\{A_k\cos\left(\frac{2\pi kE}{I}\right)+B_k\sin\left(\frac{2\pi kE}{I}\right)\right\}. \qquad (2)$$

The number of points in the expansion is defined by the binning interval $\Delta\epsilon$ and the interval I over which the excitation energy is measured, that is, $2M=I/\Delta\epsilon$.

Following the ideas of Böhning, information about the coherence width is contained in the square of the Fourier coefficients,

$$S_k=A_k^2+B_k^2. \qquad (3)$$

It is also assumed that A_k and B_k are random numbers with Gaussian distributions and that S_k has an exponential distribution. The average value of S_k is

$$\langle S_k\rangle=\left\langle\frac{d\sigma}{d\Omega}\right\rangle^2 C(0)4\pi\left(\frac{\Gamma}{I}\right)(\exp(-2\pi\Gamma k/I)+\mu). \qquad (4)$$

The parameter μ has been included in the exponential distribution to represent the "white noise" produced by the statistical errors for all values of k, and $C(0)$ is the normalized variance. Equation (4) can be rewritten as

$$\ln\langle S_k\rangle=\ln[\exp(bk+c)+\mu], \qquad (5)$$

where $b=-2\pi\Gamma/I$ and

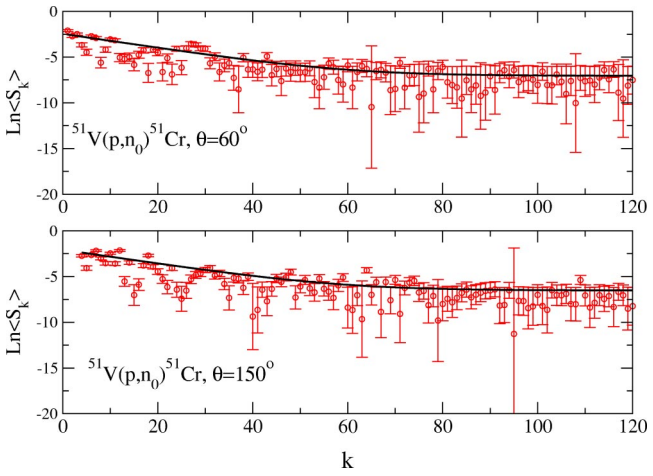

FIG. 6. $\ln\langle S_k\rangle$ and nonlinear fitting for $^{51}\mathrm{V}(p,n_0)^{51}\mathrm{Cr}$ for 60° and 150°.

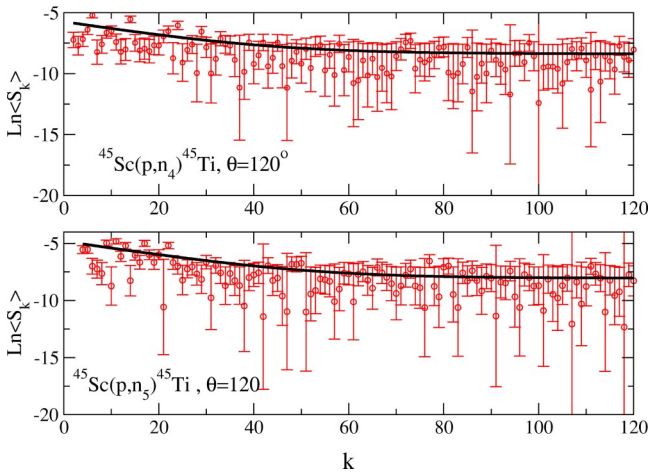

FIG. 7. $\ln\langle S_k\rangle$ and nonlinear fitting for $^{45}\mathrm{Sc}(p,n_4)^{45}\mathrm{Ti}$ and $^{45}\mathrm{Sc}(p,n_5)^{45}\mathrm{Ti}$ at 120°.

$$c = \ln\left[\left\langle \frac{d\sigma}{d\Omega}\right\rangle^2 C(0)4\pi\left(\frac{\Gamma}{I}\right)\right]. \tag{6}$$

If we consider the correction factors needed to compensate for effects of finite energy resolution [8] Eq. (5) may be expressed as:

$$\ln\langle S_k\rangle = \ln[\exp(qk^2 + bk + c) + \mu] = \ln(A_k^2 + B_k^2). \tag{7}$$

Thus, a fit to the S_k distribution as a function of k should allow us the determination of the experimental level width and its error. In principle, the magnitude of q in Eq. (7) could be calculated from the known energy resolution, however, in a time of flight measurement, the energy resolution is not constant over the entire energy range, so it was felt that allowing q to be a fitting parameter was a better means of correcting for energy resolution than setting at a given resolution.

There are also other methods of extracting experimental level widths, for example the autocorrelation method and counting the number of maxima. These three methods provide consistent results, however the Fourier method provides smaller errors [9]. The extraction of the experimental level width is done with neutron spectra measured at backward angles, as is shown in Fig. 5, where the influence of direct reactions is minimum, that is the spectra contains information dominantly of compound nuclear reactions.

A program that adopts the method of the Singular Value Decomposition [10] was used to evaluate A_k, B_k, $\ln\langle S_k\rangle$ and its errors. An excellent match was found between the experimental points for $d\sigma/d\Omega$ and the fitted values for all the samples in the analysis. The natural logarithm of the sum of the squares of the Fourier coefficients, $\ln(A_k^2+B_k^2)=\ln\langle S_k\rangle$ is plotted as a function of the index k in Figs. 6, 7, and 8. We should notice that for certain combinations of small values of A_k and B_k the errors in some of $\ln\langle S_k\rangle$ are large compared with the general trend of errors. This class of errors represents ~6% of the sample in the $\ln\langle S_k\rangle$ distribution and can be understood in terms of the error associated with $d\sigma/d\Omega$ in the Fourier expansion and the $\ln\langle S_k\rangle$ itself. It has been observed that the errors in the coefficients A_k and B_k are practically constant and independent of the index k, that is $\sigma_{A_k} \sim \sigma_{B_k}=\varepsilon$, and if we assume $A_k=B_k$ then the error for the coefficient k in $\ln\langle S_k\rangle$ reduces to $\sigma_k(\ln\langle S_k\rangle)=\pm\sqrt{2}\varepsilon/A_k$, showing that a large value of $\sigma_k(\ln\langle S_k\rangle)$ could be obtained for a combination of small values of A_k and B_k.

C. Level width in the continuum and correction for the finite range of data errors

A fitting to the $\ln\langle S_k\rangle$ distribution when the model depends nonlinearly on certain unknown parameters led to the coherence width. The coherence width obtained with the functional form of Eq. (5) and the one including corrections for the finite energy resolution, represented by Eq. (7), did not show a significant difference in the parameter having the information on the level width in the continuum, due to the good energy resolution of the experiment. The approach to solve the nonlinear problem consisted of defining a merit function χ^2 and determining the best parameters by an inter-

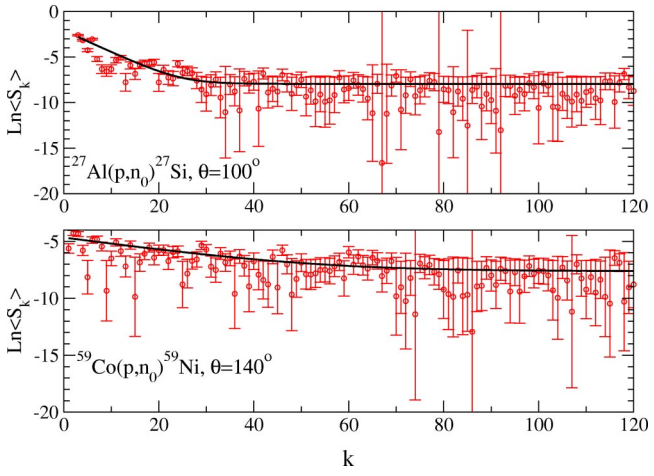

FIG. 8. $\ln\langle S_k\rangle$ and nonlinear fitting for $^{27}\mathrm{Al}(p,n_0)^{27}\mathrm{Si}$, 100° and $^{59}\mathrm{Co}(p,n_0)^{59}\mathrm{Ni}$, 140°.

TABLE II. Level width in the continuum and FRD error. The error in the coherence width is statistical proceeding from the nonlinear fitting.

Angle	I (keV)	μ	M'	M	$\Delta\Gamma_{FRD}$ (keV)	$\langle\Gamma\rangle$ (keV)
^{27}Al$(p,n_0)^{27}$Si						
100°	855	0.00035	33.9	180	±2.39	32±1
110°	879	0.00029	34.5	180	±2.38	33±1
130°	793	0.00020	30.7	170	±2.56	35±2
^{45}Sc$(p,n_4)^{45}$Ti						
120°	740	0.00023	141.0	170	±0.24	7±1
140°	857	0.00012	246.3	180	±0.12	5.0±0.7
160°	842	0.00011	197.2	180	±0.17	6.2±0.8
^{45}Sc$(p,n_5)^{45}$Ti						
120°	735	0.00032	134.5	170	±0.26	7±1
140°	822	0.00038	171.8	180	±0.20	6.0±0.9
160°	797	0.00011	218.0	180	±0.14	5.3±0.5
^{59}Co$(p,n_0)^{59}$Ni						
140°	784	0.00049	133.9	180	±0.28	7.1±0.8
150°	772	0.00035	171.5	180	±0.19	5.7±0.6
160°	778	0.00031	107.6	180	±0.38	9.3±0.8
^{51}V$(p,n_0)^{51}$Cr						
60°	760	0.00086	91.8	180	±0.48	9.3±0.4
80°	849	0.00146	100.2	200	±0.47	8.8±0.8
110°	859	0.00081	79.8	200	±0.89	12.2±0.6
150°	848	0.00147	85.5	180	±0.59	10.3±0.5
160°	855	0.00135	104.6	180	±0.44	8.6±0.5

active minimization using the Lavenberg-Marquardt method. The execution of the program with the use of all of the data points in the $\ln\langle S_k\rangle$ distribution returned an unreliable high value for χ^2; at this point we started to remove the first terms in the $\ln\langle S_k\rangle$ distribution and observe the response of the χ^2 versus the number of points removed. At some stage during this procedure a further removal did not significantly decrease the χ^2 value, leaving it practically constant. This procedure of removing is equivalent to removing the long term modulation produced by direct reactions leaving the fluctuating part which is of interest for the fluctuation analysis. Figures 6–8 show the nonlinear fitting on the $\ln\langle S_k\rangle$ distribution, and Table II presents the coherence width obtained under this procedure.

Correction for the coherence width due to the finite range of data errors (FRD) has been calculated [11] with the following expressions:

$$\Delta\Gamma_{FRD} = \pm\sqrt{\frac{3I^2}{\pi^2 M'^3}}, \tag{8}$$

$$M' = -\frac{I}{2\pi\Gamma}\ln\mu, \quad M' \leqslant M, \tag{9}$$

where it is assumed that the first M' points of the $\ln\langle S_k\rangle$ distribution fix the coherence width. Table II shows the FRD error $\Delta\Gamma_{FRD}$ calculated using expressions (8) and (9). The FRD error is not included in the error reported for the coherence width, which is only statistical, coming from the nonlinear fitting. The condition $M' \leqslant M$, given by Eq. (9), is fulfilled in all cases except for ^{45}Sc(p,n_4), $\theta = 140°, 160°$ and ^{45}Sc(p,n_5), $\theta = 160°$; however, a visual inspection of the $\ln\langle S_k\rangle$ distribution for these reactions and angles reveals values of $M' \sim 140$, 130, and 120, respectively, which are less than the quoted value of $M = 180$. The FRD error for these reactions included the recalculated values of M' in the sixth column of Table II. Finally, given that the coherence width did not show a strong angular dependence they were weighted as is shown in Table III. The error assigned to the coherence width includes the average energy resolution of 4 keV added in quadrature to the weighted error.

D. Isospin considerations

For reactions induced by protons on targets with $N > Z$, compound states with two isospins may be formed. If T is

TABLE III. Level width in the continuum for the present experiment. The error includes the average energy resolution of ⩽4 keV.

Compound nucleus	$\langle U\rangle$ (MeV)	$\langle\Gamma\rangle$ (keV)
^{28}Si	18.9	33±5
^{46}Ti	15.5	5.9±4
^{52}Cr	13.5	9.6±4
^{60}Ni	12.9	6.9±4

TABLE IV. Level widths corrected for Isospin.

Compound nucleus	Measured $\langle\Gamma\rangle$ (keV)	$\Gamma^<$ (keV)	$\Gamma^>$(keV)	$\Gamma^</\langle\Gamma\rangle$
^{28}Si	33±5	20.2±3.1	42.5	0.61
^{46}Ti	5.9±4	3.9±2.6	18.1	0.66
^{52}Cr	9.6±4	8.8±3.7	17.2	0.92
^{60}Ni	6.9±4	5.3±3.1	22.4	0.77

the isospin of the target **(**$T=(N-Z)/2$**)**, the Clebsch-Gordon coefficients for coupling to the compound state [12,13] of isospin $T-\frac{1}{2}$ and $T+\frac{1}{2}$ are $2T/(2T+1)$ and $1/(2T+1)$, respectively. If the widths of these states differ, it is shown in Ref. [14] that the observed width Γ from a fluctuation measurement will be

$$\Gamma = \frac{\sigma^<(p,n)}{\sigma(p,n)}\Gamma^< + \frac{\sigma^>(p,n)}{\sigma(p,n)}\Gamma^>, \qquad (10)$$

where Γ is the measured width, $\Gamma^<$ and $\Gamma^>$ are the widths of the $T_c=T-\frac{1}{2}$ and $T_c=T+\frac{1}{2}$ compound states, respectively, and $\sigma^>(p,n)$ and $\sigma^<(p,n)$ are the cross sections for the (p,n) reaction through $>$ and $<$ states, respectively. Finally, $\sigma(p,n)$ **(**$=\sigma^<(p,n)+\sigma^>(p,n)$**)** is the total cross section to the level.

It can be shown that for $T>1/2$ (Sc,V,Co) targets) $\Gamma^>=(1/2T)(D^>/D^<)(\Gamma_p^</\Gamma^<)\Gamma^<$ while if $T=1/2$(Al) then $\Gamma^>=\Gamma^<(D^>/D^<)$**(**$((\Gamma^<-\Gamma_\alpha^<)/(\Gamma^<)$**)**. Here, $D^>/D^<$ is the reciprocal of the ratio of level densities in the compound nucleus of $>$ and $<$, respectively. This ratio is evaluated using the conventional level density form and shifting the energy for the greater case by $E_T=96(N-Z+1)/A$. In the absence of mixing, $\sigma^>(p,n)$ would be zero if $T>1/2$. For a mixing fraction $\eta\,(0\leqslant\eta\leqslant 1)$, the ratio $\sigma^>(p,n)/\sigma(p,n)$ is $\eta/(2T+\eta)$. Based on previous studies [14], we assume $\eta=1/2$. Finally, $\sigma^>(p,n)/\sigma(p,n)$ for Al will be $(\Gamma+\Gamma_\alpha)/2\Gamma$.

Inserting these values in Eq. (10) along with the measured values of $\langle\Gamma\rangle$, we obtain the results in Table IV. The numbers in the last column give the reaction in $\Gamma^<$ compared to Γ; this again gives a correlation of one over this number to the level density.

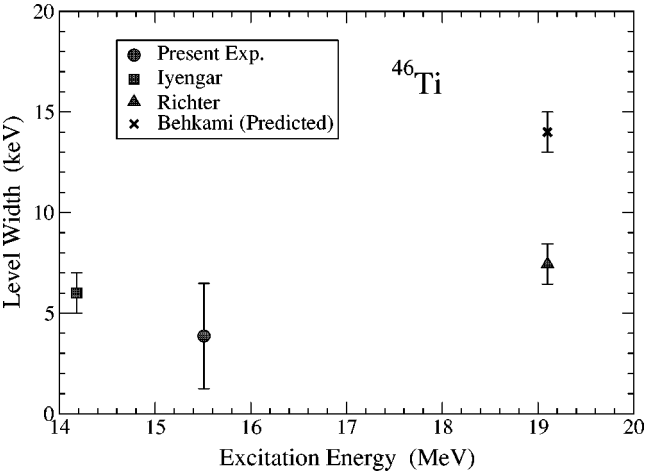

FIG. 10. Level width of ^{46}Ti.

E. Comparison with other measurements

Level widths in the continuum have been measured at different excitation energies and with different methods. Figure 9 shows the coherence width for ^{28}Si as a function of the excitation energy. Our $\Gamma^<$ width agrees very well with the local trend defined by the level widths of Elliot [15], Bubb [16], Shaw [17] and Put [18]. However, Halbert [19] who measured level widths at ~25 MeV of excitation energy through the reaction ^{12}C(^{16}O,α)^{24}Mg appears to overestimate the level width based on other measurements and in consequence, as we will discuss below, underestimates the level density.

Level widths in ^{46}Ti have been measured by Iyengar [20], Richter [21] and predicted by Behkami [22]. The predicted width of Behkami has been calculated at the same excitation energy as that measured by Richter but they differ by a factor of 2, as can be observed in Figure 10. As we know, the level

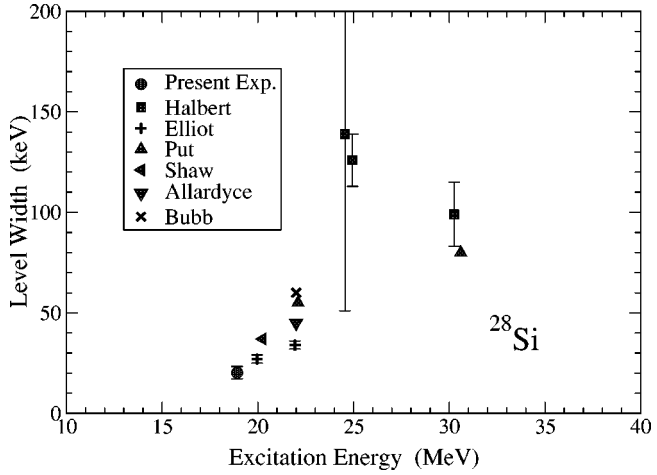

FIG. 9. Level width of ^{28}Si.

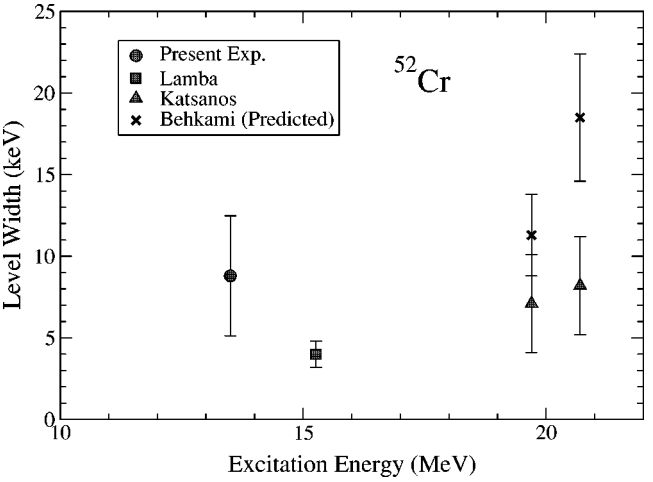

FIG. 11. Level width of ^{52}Cr.

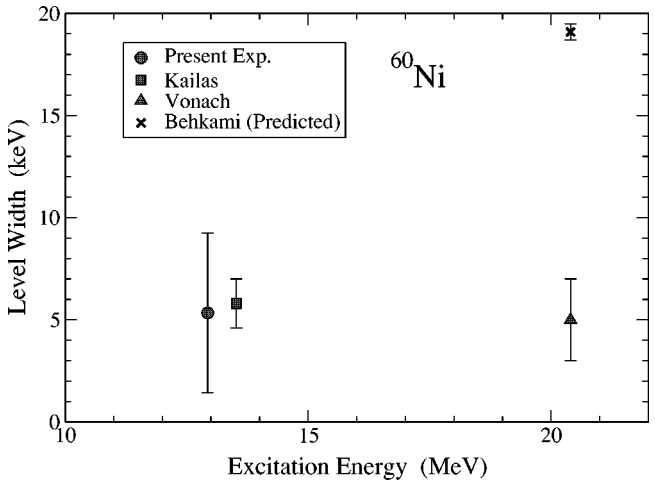

FIG. 12. Level width of ^{60}Ni.

width increases with the excitation energy because more particles can be emitted by a higher level but this trend seems not to be followed by the width measured by Richter. As we will observe later, in the discussion of level densities, if this value is low, it would result in an overestimate of the level density.

Figure 11 shows the level width as a function of the excitation energy for ^{52}Cr including the experimental values of Lamba [23], Katsanos [24] and the two predicted widths of Behkami [22], evaluated at the same excitation energy as the widths of Katsanos. We can observe that the widths of Katsanos are lower than the expected trend at ~20 MeV of excitation energy based on other measurements. The predicted width of Behkami seems to be more realistic at this energy. The level widths of Lamba and the present experiment are close in excitation energy but they differ by a factor of ~2 in the level width. Lamba measured the excitation function in steps of 5 keV but he reports a level width of 4 keV even though he claims an energy resolution of 1 keV. On the other hand, a coherence width obtained from fluctuations in a (p,p') reaction would be characteristic of the upper isospin channel for $A>50$ [12].

The fluctuation analysis of the reaction ^{59}Co$(p,n)^{59}$Ni yields a coherence energy $\langle\Gamma\rangle=(6.9\pm4)$ keV for the compound nucleus ^{60}Ni and a $\Gamma^{<}=5.3$ keV at an excitation energy of $U=12.9$ MeV. Additional measurements of the level width have been reported by Kailas [25] who studied total (p,n) reaction cross sections in ^{59}Co to extract an average level width in ^{60}Ni using the "counting of maxima" method. He obtained $\langle\Gamma\rangle=(5.8\pm1.2)$ keV at an excitation energy of $U=13.5$ MeV, that is slightly higher in energy than our measurement. Both measurements agree well considering their experimental errors, as can be observed in Fig. 12. Another measurement attributed to Vonach [26] gives a lower width value $\langle\Gamma\rangle=(5\pm2)$ keV at $U=20.4$ MeV; it was measured using the reaction ^{59}Co$(p,\alpha_{\circ})^{56}$Fe. Vonach's width seems to underestimate the trend of level width with excitation energy. The predicted width of Behkami [22], evaluated at the same excitation energy as Vonach, is a factor of 4 times greater than Vonach's width and seems to be more realistic at this excitation energy.

IV. EVALUATION OF LEVEL DENSITY

A. Level density

The density of levels of spin J and excitation energy U can be expressed as

$$\rho(U,J)=\frac{\sqrt{\pi}}{12}\frac{\exp[2\sqrt{a(U-\delta)}]}{a^{1/4}(U-\delta)^{5/4}}\times\frac{(2J+1)\exp[-(J+1/2)^2/2\sigma^2]}{2\sqrt{2\pi}\sigma^3}, \quad (11)$$

where a is the level density parameter, δ the energy shift, and σ the spin cutoff. The density of levels of a given parity π is just one half of this quantity if one assumes an equal probability of both parities which is the case at higher excitation energies [27]. The energy shift δ reflects the observed difference among level densities, $\omega(U)$, for even-even, even-odd, and odd-odd nuclei; its influence is sensitive only at low energies while opposite is valid for the level density parameter a.

The spin cutoff parameter, σ, that considers the nucleus as a rigid sphere with radius $R=1.25A^{1/3}$ and mass number A [28], is given by:

$$\sigma^2=0.0145\,A^{5/3}\sqrt{\frac{U-\delta}{a}}. \quad (12)$$

Additional approaches in describing the spin cutoff can be found in the paper of Huang [28] and Al-Quraishi [29].

To obtain the level density $\omega(U)$ at a given excitation energy, we sum $\rho(U,J)$ over J to get the observable and measurable level density:

$$\omega(U)=\sum_j \rho(U,J)\cong\int_0^{\infty}\rho(U,J)dJ, \quad (13)$$

$$\omega(U)=\frac{1}{12\sqrt{2}}\frac{e^{2\sqrt{a(u-\delta)}}}{a^{1/4}(U-\delta)^{5/4}\sigma}. \quad (14)$$

B. Experimental level density equation

It has been shown in the fluctuation theory [30] that the relation between the transmission coefficients $T_c^{J\pi}$, for the decay into different open channels c, and the average level width, of spin J and parity π, $\Gamma^{J\pi}(U)$, in the compound nucleus is:

$$2\pi\frac{\Gamma^{J\pi}(U)}{D^{J\pi}(U)}=\sum_c T_c^{J\pi}, \quad (15)$$

where the average spacing of compound levels, $D^{J\pi}(U)$, is related to the density of levels by: $\rho(U,J)=1/D^{J\pi}(U)$. According to Ericson [5],

TABLE V. Calculation of the maximum excitation energy in the residual nucleus, $U_{\max}^{\text{res}}$, for the given proton incident energy. Also shown is the maximum resolved energy level for the residual nucleus included in the HF code.

Reaction	$\langle E_p \rangle$ (MeV)	$U_{\max}^{\text{res}}$ (MeV)	Resolved level (MeV)	Needed LDP
^{27}Al$(p,n)^{27}$Si	7.40	1.80	5.208	No
^{27}Al$(p,p)^{27}$Al	7.40	7.40	5.827	Yes
^{27}Al$(p,\alpha)^{24}$Mg	7.40	9.00	9.301	No
^{45}Sc$(p,n)^{45}$Ti	5.20	2.35	1.468	Yes
^{45}Sc$(p,p)^{45}$Sc	5.20	5.20	1.662	Yes
^{45}Sc$(p,\alpha)^{42}$Ca	5.20	7.54	4.904	Yes
^{51}V$(p,n)^{51}$Cr	3.10	1.56	3.263	No
^{51}V$(p,p)^{51}$V	3.10	3.10	3.517	No
^{51}V$(p,\alpha)^{48}$Ti	3.10	4.25	3.699	Yes→No
^{59}Co$(p,n)^{59}$Ni	3.40	1.54	2.415	No
^{59}Co$(p,p)^{59}$Co	3.40	3.40	2.713	Yes→No
^{59}Co$(p,\alpha)^{56}$Fe	3.40	6.64	4.401	Yes→No

$$\sum_c T_c^{J\pi} = G(J^\pi) \cong \sum_\nu \sum_{l=0}^{\infty} \int_0^{U_\nu^{\max}} dU_\nu T_l(\epsilon_\nu) \sum_{s=|J-l|}^{J+l} \sum_{J=|S-i_\nu|}^{S+i_\nu} \rho_\nu(U_\nu, J). \tag{16}$$

The summation over ν is over all possible exit channels for a particular J, $\rho_\nu(U_\nu, J)$ is the density of levels in the residual nucleus, ϵ_ν the channel energy of the particle ν, S the channel spin of the exit channel, and i_ν the spin of the ejectile.

The coherence width $\langle \Gamma \rangle$ can be linked to the partial level width, $\Gamma^{J\pi}$, through an average procedure with some discrete probability distribution:

$$\langle \Gamma \rangle = \sum_{J\pi} P(J^\pi) \Gamma^{J\pi}. \tag{17}$$

Replacing the partial level width from Eq. (15) into Eq. (17) and considering one parity calculation, that is $G(J^-) = G(J^+) = G(J)$, $P(J^-) = P(J^+) = P(J)$, and $H(J,+) = H(J,-) = H(J)$, we obtain the level density.

$$\omega(U) = \frac{1}{\pi \langle \Gamma \rangle} \sum_J \frac{G(J)}{H(J)} P(J). \tag{18}$$

The term $H(J)$ comes from the separation of variables for the density of levels $\rho(U,J) = \omega(U) H(J,\pi)$. Equation (18) was used in the evaluation of the experimental level density in a compound nucleus. Of all the variables included in the cited equation, $G(J)$ can be evaluated with expression (16) while $H(J)$ and $P(J)$ are given below:

$$H(J) = \frac{J+1/2}{2\sigma^2} \exp\left(- \frac{(J+1/2)^2}{2\sigma^2} \right), \tag{19}$$

$$P(J) = \frac{\langle \sigma_{\alpha\alpha'} \rangle^J}{\langle \sigma_{\alpha\alpha'} \rangle} = \frac{(2J+1) \dfrac{T_\alpha^J T_{\alpha'}^J}{\sum T_{\alpha''}^J}}{\sum_J (2J+1) \dfrac{T_\alpha^J T_{\alpha'}^J}{\sum T_{\alpha''}^J}}, \tag{20}$$

where the sum in the denominator of Eq. (20) runs over all possible exit channels, that is $\Sigma T_{\alpha''}^J = G(J)$.

C. Evaluation of level densities

The calculation of level density with Eq. (18) reduces to the measurement of the coherence width $\langle \Gamma \rangle$, the knowledge of the spin cutoff parameter σ in Eq. (19), and the evaluation of expressions (16) and (20) with adequate transmission coefficients. Not only the transmission coefficients but also the density of levels in the residual nuclei give the model dependent character of the evaluation of level density in the compound nucleus. However, if the excitation energies in the residual nuclei are low, the model dependence of the density of levels can be reduced to a model independent, that is described by the resolved levels. This is the case for the level density in ^{52}Cr and ^{60}Ni for example.

The transmission coefficients $T_l(\epsilon_\nu)$ were evaluated with the FOP code [31] with a preference of local optical model parameters (OMP) to global ones; this was the case, in general, for (p,p) reactions and in some cases for (α,α) reactions; however given the scarce compilations of OMP for neutrons we resorted to global systematics of Wilmore and Hodgson [32]. The compilation of phenomenological OMP of Perey and Perey [32] was the principal source of information for these parameters.

Equation (16) was computed with the HF code [33] which may include calculations with or without isospin. From these calculations and from additional considerations, we know that $G(J^\pi)^< \sim G(J^\pi)$ and also $P(J)^< \sim P(J)$ and $H(J)^< \sim H(J)$, such that the evaluation of the level density consid-

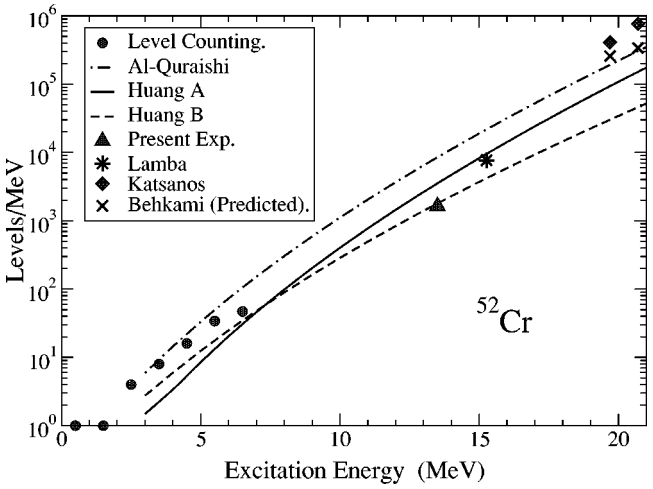

FIG. 13. Level density of ^{52}Cr.

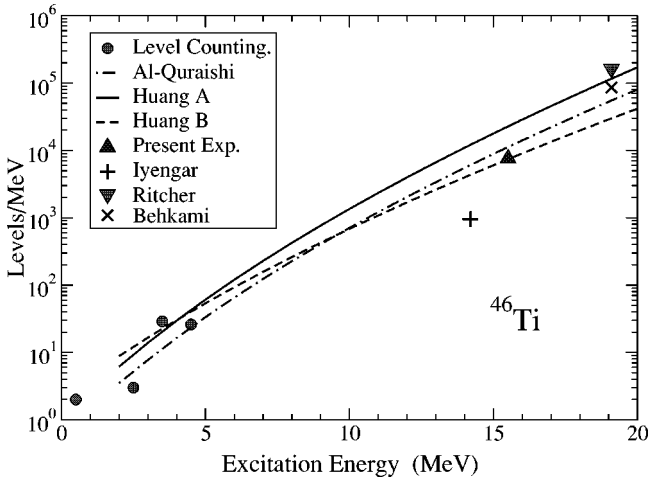

FIG. 14. Level density of ^{46}Ti.

ering the lower isospin is correlated to the values of $\Gamma^{<}/\Gamma$ shown in Table IV.

To evaluate the level density in the compound nucleus ^{52}Cr through reaction ^{51}V$(p,n)^{51}$Cr requires transmission coefficients for neutron, proton and alpha particles, which are the only possible decay channels from ^{52}Cr into the different residual nuclei for the average proton energy shown in Table V. The proton transmission coefficients were evaluated with the reaction ^{51}V$(p,p)^{51}$V with the OMP of Prokopenko [34] while for the reaction ^{48}Ti$(\alpha,\alpha)^{48}$Ti the OMP of Satchler [35] was chosen. The neutron transmission coefficients were calculated with the reaction ^{51}Cr$(n,n)^{51}$Cr with the global OMP of Wilmore and Hodgson. Different sets of OMP were also tested to observe the variations not only in the transmission coefficients but also in the level densities. For the present range of kinetic energies we observed that the transmission coefficients follow the inequality $T_l^n > T_l^p > T_l^\alpha$, which is an important consideration in the calculation of expression (16). Table V shows the maximum excitation energy reached by residual nuclei ^{51}Cr, ^{51}V, and ^{48}Ti and also the maximum resolved level, input to the HF code, for the evaluation of the density of levels $\rho(U,J)$. Given that the resolved levels extend higher in energy than the maximum excitation energy in ^{51}Cr and ^{51}V no level density parameters (LDP) are needed for these nuclei in the evaluation of expression (16). The opposite view is valid for ^{48}Ti but given the low values for T_l^α the contribution of this alpha decay channel is practically eliminated resulting in a level density in ^{52}Cr independent of the level density model in the residual nuclei. The level density for ^{52}Cr is shown in Fig. 13.

The compound nucleus ^{46}Ti was excited up to an excitation energy of $\langle U\rangle = 15.5$ MeV; from energy considerations, the residual nuclei ^{45}Ti, ^{45}Sc, ^{42}Ca, and ^{38}Ar can be formed by the emission of a neutron, proton, alpha and two alphas, respectively. However, given the low kinetic energy involved in the 2α decay and its low transmission coefficient, this decay can be eliminated from the calculation. The proton transmission coefficients were calculated with the OMP of Prokopenko [34] while the OMP of Jackson [36] was used for the α-channel. The transmission coefficients follow the inequality relation, $T_l^n > T_l^p \sim T_l^\alpha$ for the range of ejectile particles. Figure 14 shows the level density for ^{46}Ti.

The level density in ^{28}Si was calculated with the OMP of Hoare [37] for protons and So [38] for alphas. For the range of the ejectile particles in consideration we found that the alpha transmission coefficients were higher than protons and neutrons, that is, $T_l^\alpha \geqslant T_l^p > T_l^n$, however, from Table V, LDP were needed only for ^{27}Al. The level density for ^{28}Si is shown in Figure 15, and was calculated including isospin.

The level density in ^{60}Ni, shown in Fig. 16, was calculated with the OMP of Prokopenko [39] for protons, and Lemos [40] for alpha particles. The transmission coefficients for the decay channels constituted by neutrons, protons and alphas are such that $T_l^n \gg T_l^p \sim T_l^\alpha$, leaving neutrons as the most important decay channel. Moreover, considering Table V we conclude that the level density in ^{60}Ni is independent of the model for the density of levels of Eq. (16).

D. Comparison with other evaluations, level density systematics, and discussion

Nuclear level densities were also calculated for the experimental and evaluated level widths shown in Figs. 9–12 following the same procedures described in a previous sec-

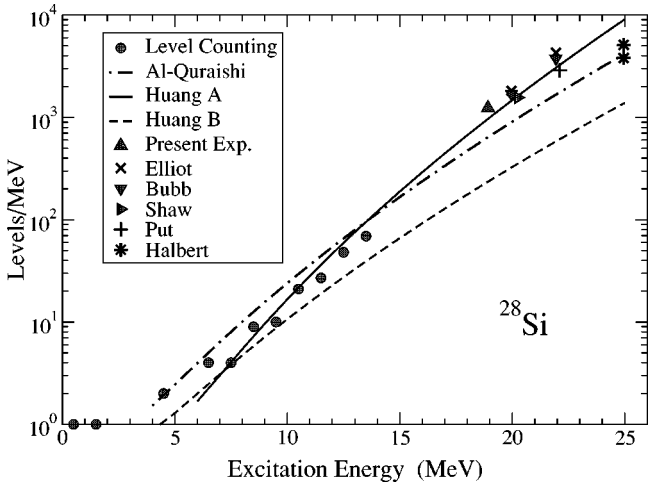

FIG. 15. Level density of ^{28}Si.

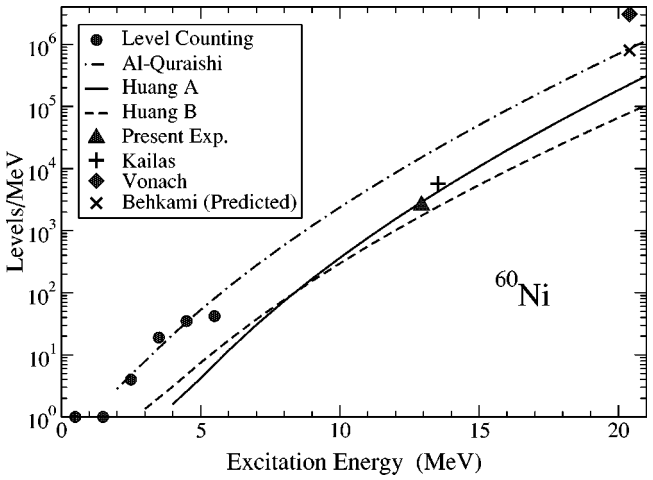

FIG. 16. Level density of ^{60}Ni.

tion. However, considering excitation energies higher than our measurements in the computation of the NLD, they are model dependent from both transmission coefficients and density of levels. NLD parameters were obtained from the systematics of Al-Quraishi [29] and we used a solid sphere spin cutoff with energy dependence. The results are shown in Figs. 13–16 where we also include the NLD systematics of Al-Quraishi [29] and Huang [28].

Reasonable agreements are found for the NLD systematics of Huang B [28] and Al-Quraishi [29] for ^{46}Ti, Huang B for ^{52}Cr, and Huang A for ^{28}Si given an estimated uncertainty of 40% in the evaluated NLD. We included the NLD compilation of Huang [28] even though his study is limited to the range of $20 \leqslant A \leqslant 41$.

As can be observed from figures of level widths and level densities, a lower coherence width produces a higher level density and *vice versa*. This is the case for the widths of Katsanos [24] in ^{52}Cr, Richter [21] in ^{46}Ti, Halbert [19] at 25 MeV in ^{28}Si, and Vonach [26] in ^{60}Ni. We realize that the NLD calculated with the experimental width of Katsanos [24] and the predicted width of Behkami [22] overestimate the NLD in ^{52}Cr, and this NLD is better represented by a combination of the level counting, the experimental point of Lamba [23] and the present experimental value. The NLD parameters, obtained from a nonlinear fitting to these selected experimental points, give $a=4.8$ and $\delta=0.3$, $3 \leqslant U \leqslant 20$. For ^{46}Ti Richter [21] appears to underestimate the level width, and as a consequence, overestimate the NLD at 19.1 MeV; the recommended NLD parameters are $a=4.8$ and $\delta=-0.3$, $3 \leqslant U \leqslant 20$ MeV. The NLD parameters for ^{28}Si, excluding the experimental points of Halbert [19] give $a=3.5$ and $\delta=4.0$, $7 \leqslant U \leqslant 25$ MeV.

There are two additional measurements of level widths in ^{60}Ni using Ericson fluctuations, one by Kailas [25] at 13.5 MeV and the other by Vonach [26] at 20.4 MeV. As we mentioned before, Vonach seems to underestimate the trend of level widths as a function of the excitation energy and as a consequence overestimates the level density; the evaluated level width of Behkami [22] calculated at the same energy of 20.4 MeV is four times greater than Vonach's width. Other evaluations of level densities in ^{60}Ni have been done by Huizenga [41] and Fisher [42]; their reported values agree with the systematics of Al-Quraishi [29]. Huizenga has studied reactions ^{59}Co$(p,\alpha_{0,1,2})^{56}$Fe and ^{56}Fe$(p,\alpha_0)^{59}$Co with a 50 keV energy resolution, evaluating the NLD with the expression $\Gamma/D_{0,\pi}$ with a model that includes the Hausser-Feshbach equation, $D_{J,\pi}$, and the measured differential cross section to the residual nucleus $d\sigma_{ab}/d\Omega$. Certainly $\Gamma/D_{0,\pi}$ is energy dependent and one of the NLD was evaluated using Vonach's level width at 20.4 MeV, while other NLD's, from $\sim$16 to 22 MeV, were evaluated with a model dependent expression of Eq. (15). It might have been possible that Huizenga [41] could have used the Vonach's [26] width as a reference in his evaluations of NLD in ^{60}Ni. If this were the case, then its level densities could be lower than the reported ones.

We also subjected our ^{60}Ni data to a "peak counting" method to extract level widths, and the results are consistent with the Fourier method. Observing a discrepancy among the data for NLD in ^{60}Ni, we suggest a more detailed study of this single magic ($Z=28$) and even-even nucleus.

[1] W. B. Howard, S. M. Grimes, T. N. Massey, S. I. Al-Quraishi, D. K. Jacobs, C. E. Brient, and J. C. Yanch, Nucl. Sci. Eng. **138**, 145 (2001).
[2] T. N. Massey, S. Al-Quraishi, C. E. Brient, J. F. Guillemette, S. M. Grimes, D. Jacobs, J. E. O'Donnell, J. E. Oldendick, and R. T. Wheeler, Nucl. Sci. Eng. **129**, 175 (1998).
[3] S. M. Grimes (private communication, Ohio University Accelerator Laboratory, 2002).
[4] J. F. Ziegler and J. P. Biersack, http://www.srim.org, 2000.
[5] T. Ericson, Ann. Phys. (N.Y.) **23**, 390 (1963).
[6] G. Deconninck and J. Royen, Nucl. Instrum. Methods **75**, 266 (1969).
[7] A. Richter, *Nuclear Spectroscopy and Reactions, Part B*, edited by Joseph Cerny (Academic Press, New York, 1974), p. 372.
[8] S. M. Grimes, Report No. INPP 1995-01, Ohio University, 1995.
[9] W. P. Abfalterer, R. W. Finlay, and S. M. Grimes, Phys. Rev. C **62**, 064312 (2000).
[10] W. H. Press, S. A. Teukolsky, W. T. Vetterling, and B. P. Flannery, *Numerical Recipes in C: General Linear Least Squares*, 2nd ed. (Cambridge University Press, Cambridge, 1974), p. 671.
[11] J. Ernst, H. L. Harney, and K. Kotajima, Nucl. Phys. **A136**, 87 (1969).
[12] S. M. Grimes, J. D. Anderson, A. K. Kerman, and C. Wong, Phys. Rev. C **5**, 85 (1972).
[13] D. Robson, A. Richter, and H. L. Harney, Phys. Rev. C **8**, 153 (1973).
[14] C. R. Lux, N. T. Porile, and S. M. Grimes, Phys. Rev. C **15**,

1308 (1979).
[15] R. V. Elliot and R. H. Spear, Nucl. Phys. **84**, 209 (1966).
[16] I. F. Bubb, J. M. Poate, and R. H. Spear, Nucl. Phys. **65**, 655 (1965).
[17] R. W. Shaw, A. A. Katsanos, and R. Vandenbosch, Phys. Rev. **184**, 1089 (1969).
[18] L. W. Put, J. D. A. Roeders, and A. Van der Woude, Nucl. Phys. **A112**, 561 (1968).
[19] M. L. Halbert, F. E. Durham, C. D. Moak, and A. Zucker, Nucl. Phys. **47**, 353 (1963).
[20] K. V. K. Iyengar, S. K. Gupta, K. K. Sekharan, M. K. Mehta, and A. S. Divatia, Nucl. Phys. **A96**, 521 (1967).
[21] A. Richter, A. Bamberger, P. Von Brentano, T. Mayer-Kuckuk, and W. Von Witsch, Z. Naturforsch. A **21a**, 1001 (1966).
[22] A. N. Behkami and S. I. Najafi, J. Phys. G **6**, 685 (1980).
[23] C. M. Lamba, N. Sarma, N. S. Thampi, D. K. Sood, and V. K. Deshpande, Nucl. Phys. **A110**, 111 (1968).
[24] M. G. Braga Marcazzan and L. Milazzo Colli, Energ. Nucl. (Milan) **15**, 186 (1968).
[25] S. Kailas, S. K. Gupta, M. K. Mehta, S. S. Kerekatte, L. V. Namjoshi, N. K. Ganguly, and S. Chintalapudi, Phys. Rev. C **12**, 1789 (1975).
[26] H. K. Vonach and J. R. Huizenga, Phys. Rev. **138**, B1372 (1965).
[27] S. M. Grimes, J. Nucl. Sci. Technol. **2**, 709 (2002).
[28] P.- L. Huang, S. M. Grimes, and T. N. Massey, Phys. Rev. C **62**, 024002 (2000).
[29] S. I. Al-Quraishi, S. M. Grimes, T. N. Massey, and D. A. Resler, Phys. Rev. C **63**, 065803 (2001).
[30] P. A. Moldauer, Rev. Mod. Phys. **36**, 1079 (1964).
[31] F. S. Dietrich, FOP-code, Lawrence Livermore National Laboratory, 1995.
[32] C. M. Perey and F. G. Perey, At. Data Nucl. Data Tables **17**, 1 (1976).
[33] S. M. Grimes, J. D. Anderson, J. W. McClure, B. A. Pohl, and C. Wong, Phys. Rev. C **10**, 2373 (1974).
[34] V. S. Prokopenko, V. V. Tokarevskii, and V. N. Shcherbin, Bull. Acad. Sci. USSR, Phys. Ser. (Engl. Transl.) **34**, 116 (1971).
[35] G. R. Satchler, Nucl. Phys. **70**, 177 (1965).
[36] D. F. Jackson and C. G. Morgan, Phys. Rev. **175**, 1402 (1968).
[37] D. Hoare, A. B. Robbins, and G. W. Greenlees, Proc. Phys. Soc. London **77**, 830 (1961).
[38] S. S. So, C. Mayer-Boricke, and R. H. Davis, Nucl. Phys. **84**, 641 (1966).
[39] V. S. Prokopenko, A. S. Klimenko, N. N. Pucherov, and V. I. Chirko, Bull. Acad. Sci. USSR, Phys. Ser. (Engl. Transl.) **34**, 113 (1970).
[40] O. F. Lemos, Orsay, Report No. 136, 1972.
[41] J. R. Huizenga, H. K. Vonach, A. A. Katsanos, A. J. Gorski, and C. J. Stephan, Phys. Rev. **182**, 1149 (1969).
[42] R. Fischer, G. Traxler, M. Uhl, and H. Vonach, Phys. Rev. C **30**, 72 (1984).